

Article

Fine-tuning Strain and Electronic Activation of Strain-promoted 1,3-Dipolar Cycloadditions with Endocyclic Sulfamates in SNO-OCTs

Eileen G. Burke, Brian Gold, Trish T. Hoang, Ronald T Raines, and Jennifer M Schomaker

J. Am. Chem. Soc., **Just Accepted Manuscript** • Publication Date (Web): 15 May 2017

Downloaded from <http://pubs.acs.org> on May 15, 2017

Just Accepted

“Just Accepted” manuscripts have been peer-reviewed and accepted for publication. They are posted online prior to technical editing, formatting for publication and author proofing. The American Chemical Society provides “Just Accepted” as a free service to the research community to expedite the dissemination of scientific material as soon as possible after acceptance. “Just Accepted” manuscripts appear in full in PDF format accompanied by an HTML abstract. “Just Accepted” manuscripts have been fully peer reviewed, but should not be considered the official version of record. They are accessible to all readers and citable by the Digital Object Identifier (DOI®). “Just Accepted” is an optional service offered to authors. Therefore, the “Just Accepted” Web site may not include all articles that will be published in the journal. After a manuscript is technically edited and formatted, it will be removed from the “Just Accepted” Web site and published as an ASAP article. Note that technical editing may introduce minor changes to the manuscript text and/or graphics which could affect content, and all legal disclaimers and ethical guidelines that apply to the journal pertain. ACS cannot be held responsible for errors or consequences arising from the use of information contained in these “Just Accepted” manuscripts.

Fine-tuning Strain and Electronic Activation of Strain-promoted 1,3-Dipolar Cycloadditions with Endocyclic Sulfamates in SNO-OCTs

Eileen G. Burke,^{1†} Brian Gold,^{1†} Trish T. Hoang,² Ronald T. Raines,^{1,2} Jennifer M. Schomaker^{*,1}

Department of Chemistry¹ and Department of Biochemistry² University of Wisconsin, Madison, Wisconsin 53706, United States

Supporting Information Placeholder

ABSTRACT: The ability to achieve predictable control over the polarization of strained cycloalkynes can influence their behavior in subsequent reactions, providing opportunities to increase both rate and chemoselectivity. A series of new heterocyclic strained cyclooctynes containing a sulfamate backbone (SNO-OCT) were prepared under mild conditions by employing ring expansions of silylated methyleneaziridines. SNO-OCT derivative **8** outpaced even DIFO in a 1,3-dipolar cycloaddition with benzylazide. The various orbital interactions of the propargylic and homopropargylic heteroatoms in SNO-OCT were explored both experimentally and computationally. The inclusion of these heteroatoms had a positive impact on stability and reactivity, where electronic effects could be utilized to relieve ring strain. The choice of the heteroatom combinations in various SNO-OCT significantly affected the alkyne geometries, thus illustrating a new strategy for modulating strain *via* remote substituents. Additionally, this unique heteroatom activation was capable of accelerating the rate of reaction of SNO-OCT with diazoacetamide over azidoacetamide, opening the possibility of further method development in the context of chemoselective, bioorthogonal labeling.

Introduction and background.

The development of reactions that display bioorthogonal behavior has enabled the study of an array of biomolecules, including proteins, lipids, and glycans, in living systems.¹ Important features of bioorthogonal reactions include selectivity between endogenous functional groups, lack of reactivity towards the native biological system, fast reaction kinetics and ease of preparation/incorporation of the chemical reporters into the desired biomolecules.¹ A handful of reaction classes are well-suited to fulfill these requirements, including the Staudinger ligation,² 1,3-dipolar cycloadditions of azides,^{3,4} diazo compounds,⁵ nitrones⁶ or nitrile imines,⁷ oxime or hydrazone formation,⁸ esterifications,^{5g,9} tetrazine ligations¹⁰ and others.¹¹

One of the most widely employed reactions in bioorthogonal chemistry is the copper-catalyzed azide-alkyne cycloaddition (CuAAC); however, the associated toxicity of the metal towards biological systems has inspired the search for alternative approaches.^{1,12} The introduction of ring strain into the cycloalkyne coupling partner was one strategy to meet this need by enabling rapid 1,3-dipolar cycloadditions with azides in the absence of a metal catalyst (Figure 1A).^{3,13} Since this initial report, strained alkynes have found utility in a range of applications beyond biological labeling, including the manipulation of proteins,¹ materials

chemistry,¹⁴ and as synthetic building blocks.¹⁵ However, despite their successes, key challenges remain in the synthesis, stability, and chemoselectivity of highly strained cycloalkynes, including ways to easily increase their water solubility for biological applications. Herein, we describe the synthesis, reactivity and computational studies of a set of new strained cycloalkynes and detail how their unique features offer advantages over traditional cycloalkynes.

The typical strategy for increasing the rates of strain-promoted azide-alkyne cycloaddition (SPAAC) reactions is to augment ring strain through the inclusion of sp²-hybridized centers (e.g. DIBO,^{3b} DIBAC,^{3c} BARAC,^{3d} and DIBONE,^{3f} Figure 1B) or small rings (BCN).^{3e} These modifications have led to improvements in reaction rates that are two orders of magnitude faster than the corresponding unactivated cyclooctynes. However, increasing the strain also destabilizes the ring, leading to unwanted reactivity with thiols and incompatibility with certain reaction conditions that limit potential applications of these cycloalkynes in biological systems.¹⁶

In contrast, the electronic activation of cyclic alkynes⁴ allows for increased rates, while effectively decreasing strain in the starting alkyne,^{4e} an approach with the potential to minimize undesired side reactions (Figure 1C). Previous examples of electronic activation have capitalized on hyperconjugative $\pi \rightarrow \sigma^*_{C-X}$ interactions.^{4e,17} These orbital interactions are especially important contributors in the transition state (TS); the placement of heteroatoms, such as O, N and S, in the propargylic position has been demonstrated to lower the ΔE^\ddagger of azide-alkyne cycloadditions.^{4e,17} For example, DIFO, an alkyne with two exocyclic propargyl fluorines, shows rate enhancements of ~30-fold in reactions with PhCH₂N₃, despite the gauche alignment of the participating orbitals.^{4a} Computational analyses of DIFO analogs carried out by Gold et al. found that rings containing endocyclic heteroatoms, where the participating orbitals display an *antiperiplanar* orientation, had a predicted ΔE^\ddagger that was 1.3 kcal/mol lower in energy than that of DIFO.^{4e,17} Medium-sized cycloalkynes with heteroatoms embedded at the propargylic positions were recently synthesized by Tomooka and co-workers, and separately by Yamamoto and co-workers, to target these orbital interactions. In the case of the Tomooka alkynes, they were found to have cycloaddition rates ~4-fold faster than cyclooctyne.^{17c} However, the reported synthetic routes were not flexible enough to accommodate smaller ring sizes, and the lower strain energies present in the accessible cycloalkynes prevented reaction rates in the addition to benzyl azide from surpassing those of DIFO.

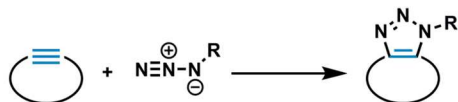
Another challenge in the synthesis of new cycloalkynes for applications in bioorthogonal chemistry is identifying ways to

modulate the polarizability of the alkyne in a manner that enables chemocontrol in cycloadditions involving two different 1,3-dipoles. Diazo compounds have proven useful in this regard, as the greater nucleophilic character of this group promotes rapid reaction rates and chemoselective transformations in the presence of azides.⁵ Cycloalkynes that exhibit the ability to further tune for selective reactivity of a diazo over an azide group are of great interest for applications in chemical biology to meet the demand for “orthogonal–bioorthogonal” reactions in bioconjugation and chemical reporter strategies.¹

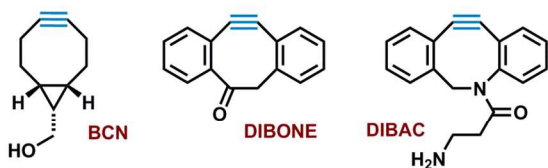
When comparing the strategies of increased strain and electronic activation to improve the reactivity of a cycloalkyne, it is obvious

Figure 1. Strain and electronic effects on rate and selectivity of strain-promoted 1,3-dipolar-alkyne cycloadditions.

A. Strain Promoted Azide–Alkyne Cycloaddition (SPAAC)

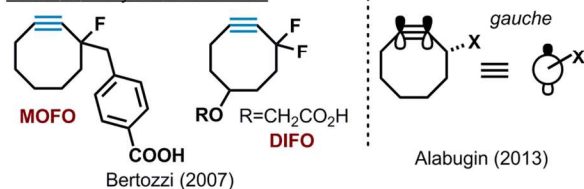


B. Strain Activation

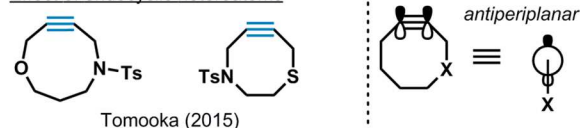


C. Electronic Activation

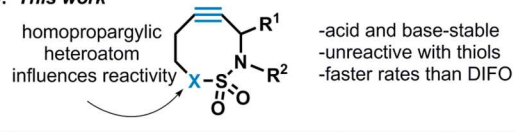
Effect of exocyclic heteroatoms



Effect of endocyclic heteroatoms



D. This work



that each approach has its own distinct advantages. When strain alone is utilized, the increasing reaction rate results in a loss of selectivity. This can be explained *via* a Hammond–Leffler type analysis, where increasing strain predistorts the cycloalkyne to not only resemble the azide cycloaddition TS, but the TS of cycloaddition TSs with other dipoles.^{5e} On the other hand, electronic effects provide for better matching between frontier molecular orbitals (FMOs), generating more rapid reactivity and higher selectivity.¹⁸ This strategy provides advantages not just in terms of preventing unwanted side reactions, but also allows for the development of mutually orthogonal chemistries.^{1,5,19} Advances in our ability to predictably tune the electronics of the dipolarophile could enable even better matching between the FMOs of the cycloalkyne and the desired 1,3-dipole.

[Type here]

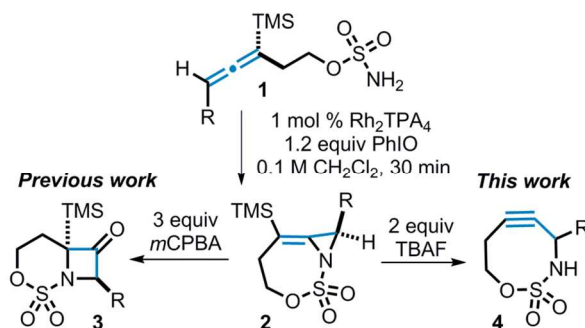
While the use of electronic activation in strained alkynes has achieved impressive increases in rate enhancements of 1,3-dipolar cycloaddition reactions, its full potential will be realized only with further efforts directed towards balancing stability and reactivity. We were curious if combining the electronic effects of propargylic and homopropargylic heteroatoms in a strained cycloalkyne might offer advantages in terms of reactivity, stability and tunability compared to similar scaffolds containing only propargyl heteroatoms. In this paper, we describe the successful development of a strategy for the efficient synthesis of a new class of cycloalkynes for chemoselective cycloaddition reactions and report computational studies of important orbital interactions that control the polarizability, relative reaction rate and reactivity of the alkyne (Figure 1D).

Results and Discussion.

Synthesis of strained cycloalkynes. One of the ongoing challenges with the use of strained cycloalkynes has been the length and inflexibility of current syntheses, owing in part to the difficulty of overcoming entropic disadvantages inherent to forming strained rings.³ In an alternate approach to these motifs, our route to heterocyclic strained alkynes capitalizes on a unique ring expansion strategy (Scheme 1).²⁰ Beginning with readily accessible silylated allenes **1**, a regio-, chemo- and stereocontrolled Rh-catalyzed aziridination forms the key endocyclic methyleneaziridine intermediate **2**. The silyl group plays a key role in directing the regioselectivity of the aziridination to the distal allene bond, due to the ability of silicon to engage in hyperconjugative stabilization of the developing positive charge, as well as by the steric bulk of the trimethylsilyl (TMS) group.²¹ In our previous work, we reported that the remaining alkene of the stable and isolable **2** undergoes diastereoselective epoxidation, followed by rapid rearrangement to furnish azetidin-3-ones of the general structure **3**.²² However, in the context of this work, it was discovered that treatment of **2** with tetrabutylammonium fluoride (TBAF) triggered elimination of the silyl group, followed by ring-opening of the aziridine, to yield the stable strained alkyne **4** (SNO-OCT) in 89% yield, with heteroatoms incorporated into the ring both at the propargylic and homopropargylic positions.

Two attractive features of this chemistry are the ability to carry out the synthesis in a single pot starting from the silylated allene **1**, as well as the ease of modifying **1** to readily deliver other useful analogs of **4**. These features are particularly useful when in-

Scheme 1. Strained heterocycles from silylated allenes.



creased solubility is desired for biological applications, as our strategy enables the ready introduction of polar functional groups into the cycloalkyne. Calculations of the log *P* of known cycloalkynes (Figure 1) and our new SNO-OCTs (Scheme S1 in the Supporting Information) show promise for the ability of our synthetic

approach to furnish more water-soluble derivatives. In addition to the flexibility inherent in the actual synthesis, the sulfamate-derived cycloalkynes display excellent thermal stability, with the standard substrate **5** showing no significant decomposition after heating at 50 °C for 18 h. The alkyne **5** did not decompose upon exposure to either trifluoroacetic acid (TFA) or aqueous NaOH for 18 h, stability attributed to lessened strain in the ring due to the inclusion of heteroatoms in the ring.^{4e,17} Finally, alkyne **5** remained inert to reaction when stirred in a pH 7 solution of 150 mM reduced glutathione over 24 h, a promising indicator of useful biorthogonality (see Figure S1 in the SI for more details).

Experimentally determined reactivity of SNO-OCTs with benzyl azide. Noting the improved stability and the previously unreported substitution pattern of sulfamate-derived cycloalkynes, we were interested in exploring the potential of these molecules for biological labeling. In addition to stability, useful alkynes for biorthogonal applications must exhibit fast rates of reaction with azides at low concentrations that mimic those found in biological settings.¹ In order to assess the reactivity of our new cycloalkynes (SNO-OCT) and enable comparisons with previously reported alkynes, the second order rate constants (k_2) for reaction with benzyl azide were measured in acetonitrile at ambient temperature using ¹H-NMR spectroscopy (Table 1, see the Supporting Information for more details). Alkyne **5**, bearing an *n*-pentyl side chain, was chosen as the 'standard' substrate, and its second-order rate constant determined to be 0.026 M⁻¹s⁻¹. To assess the impact of electronic manipulation on the reaction rate, a series of analogs were synthesized and their k_2 values compared to the k_2 value of **5** to give a k_{rel} value, as indicated in Table 1.

Modifications to the scaffold of **5** led, in some cases, to dramatic changes in the observed rates. While N-Boc protection of the propargylic N to furnish **6** resulted in similar reactivity as compared to **5**, substitution of the homopropargylic O of **5** for the NBoc group of **7** gave a k_2 value significantly lower than that of **5**. Increasing the electrophilicity of the exocyclic C–C bond through addition of an alcohol in **8** tripled the k_2 value, giving the fastest rate of reaction with any of the sulfamate-derived cycloalkynes studied thus far.

Comparison of rates to existing alkynes. As compared to previously reported alkynes, the new SNO-OCT cycloalkynes react with benzyl azide at competitive rates (Table 1A). When compared to OCT (Table 1B), compounds **5**, **6** and **8** react substantially faster, generally by an order of magnitude. Alkynes that rely on high ring strain to increase reactivity, such as BCN, DIBONE and DIBAC, have the highest reported rates for cycloalkynes. However, testing **8** in CD₃OD or 2:1 D₂O:CD₃CN for direct comparison with these known alkynes revealed that the rate of reaction with PhCH₂N₃ is on the same order of magnitude as BCN, DIBONE and DIBAC. When compared to electronically activated alkynes, the sulfamate cycloalkynes **5**, **6** and **8** were faster than the exocyclic activated MOFO, and **8** was faster than DIFO. Cycloalkyne **8** was also substantially faster than the alkynes bearing two endocyclic propargylic heteroatoms reported by Tomooka, despite the fact that SNO-OCT contains only one propargylic heteroatom. This result was especially intriguing, as the single propargylic heteroatom in SNO-OCT is the nitrogen of the sulfamate, a weak σ -acceptor compared to the propargylic oxygen atoms utilized by Tomooka^{17c} and the exocyclic fluorines in DIFO.^{4a} To better understand the influence of the propargyl and homopropargyl heteroatoms on the reaction rate, as well as provide insight for the design of analogs with even greater reactivity, computational analyses of sulfamate-derived cycloalkynes were carried out.

Computational analysis of sulfonyl inclusion. While experimental results demonstrate the dramatic effect of introducing the

sulfonyl functionality into the ring on the reactivity of our new cycloalkynes, determining which factors contribute to the observed effect is challenging. Computationally, the reactivity of an octyne derivative containing a homopropargylic sulfonyl group **11** with MeN₃ was compared to the same reaction of the parent cyclooctyne **9** with MeN₃ (Figures 2A–B). It was found that the

Table 1. Comparison of the second-order rate constants (k_2) for alkyne-azide cycloaddition in different solvents.

A. Sulfamate-containing cycloalkynes (SNO-OCT)			
$k_2 = 0.025 \text{ M}^{-1}\text{s}^{-1}$	0.023	0.0014	$0.087, 0.13, 0.13$
$k_{rel} = 1.0$	0.92	0.056	3.5
B. Comparison to reported alkynes			
$k_2 = 0.0024 \text{ M}^{-1}\text{s}^{-1}$	0.29	0.26	0.31
	Strain Activation		Electronic Activation
		0.0085	0.076
		0.0085	0.019

inclusion of the sulfonyl moiety relaxes the alkyne bond angles from 158°/159° in the cyclooctyne **9** (X = Y = CH₂) to 161°/161° in **11** (X = Y = CH₂). The fact that increased rates were observed for **5**–**8**, despite the potential relaxation of the ring strain, suggests that electronic effects must play a significant role in the increased reactivity. Comparison with the Tomooka alkynes (Figure 1), which display similar bond angles of 162°/160°, but k_2 values an order of magnitude slower than **8**, suggests that there must be some other effect operating that goes beyond activation by the single propargyl heteroatom. Additionally, NBO calculations on scaffolds based on **11/12** (Figure 2) show a more polar TS in the cycloaddition reaction due to inductive effects and double hyperconjugation through exocyclic C–C propargylic bonds (see the SI for full details). With these preliminary results in mind, further computational studies were undertaken to develop an understanding of the role of individual heteroatoms on the reactivity.

First, the effect of the propargyl heteroatom was isolated by replacing the homopropargylic oxygen (Y) with a methylene unit to furnish **9** and **11** (Figure 2A–B). The remaining X atom was varied from CH₂ to NH to O to NH₂⁺, both with and without the endocyclic sulfonyl group. Surprisingly, incorporation of the sulfonyl moiety led to deviations in the previously reported trend of increased reactivity as the acceptor ability of the X atom is increased.^{4e,17} A hint to the origin of this effect was revealed by distortion/interaction analysis,⁵³ where large distortion energies were required to reach the TS when X or Y = NH₂⁺, especially for the sulfonyl containing alkynes **11c** and **12c** (Figure 2D). Examining starting geometries reveals substantial relaxation of alkyne angles and a significantly lengthened S–N bond upon protonation (Figure 2C). This trend is readily explained by Bent's rule, where bond lengths were found to increase with increasing p-character.²⁴ Calculated S–NH₂⁺ bond lengths of 1.88 Å and 1.89 Å are observed in **11c** and **12c**, respectively, versus much shorter S–NH

[Type here]

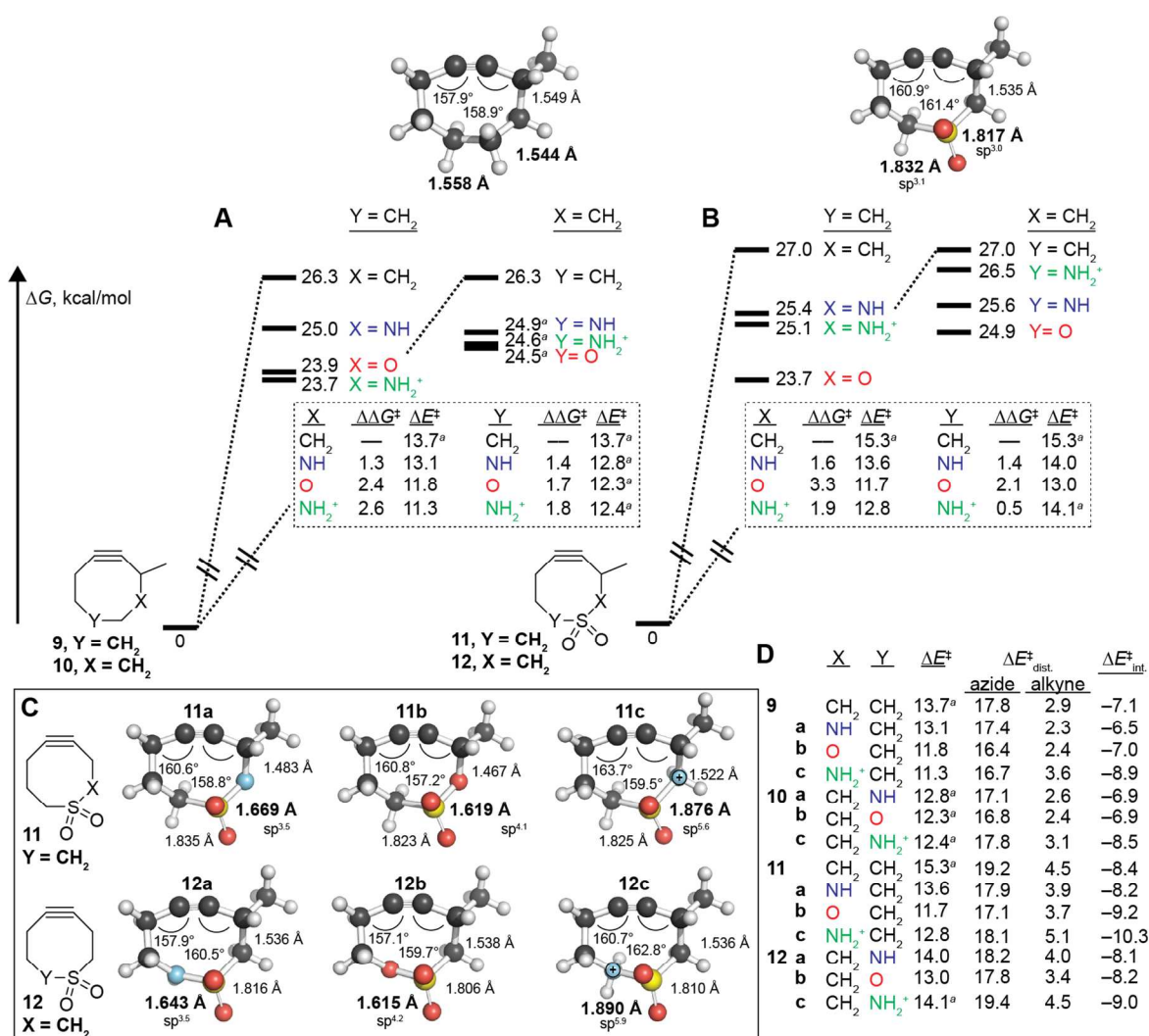


Figure 2. Calculated free energies (M06-2X/6-311+G(d,p) level of theory with an IEFPCM solvent model for water (radii = UFF)) of activation (kcal/mol) of the lowest energy TSs for cycloaddition of methyl azide with alkynes containing various propargylic and homopropargylic substituents either without an endocyclic sulfonyl group (**A**) or containing an endocyclic sulfonyl group (**B**). (**C**) Starting alkyne geometries with selected bond lengths given in Ångstroms and angles in degrees. Hybridizations were obtained from NBO analyses²⁶ for the sulfur bonding orbitals in S–X and S–Y bonds. Black = carbon; white = hydrogen; blue = nitrogen; red = oxygen; yellow = sulfur. (**D**) Distortion/interaction analysis. For a full analysis and further computational details, see Table S6 in the Supporting Information. ^aThe *syn* TS is preferred. *Syn* refers to the relationship of the azide methyl group relative to the C–X bond.

bond lengths of 1.67 Å and 1.64 Å for compounds **11a** and **12a**, respectively. Compared to the S–C length of 1.82 Å for the parent compound **11** (X = Y = CH₂), it is noted that incorporation of neutral heteroatoms (**11/12a** and **b**) decrease the S–X or S–Y bond length, but protonation leads to an increase. In addition to hybridization effects, anomeric effects were also found to influence the S–X bond length.²⁵ The *endo*-anomeric effect ($n_X \rightarrow \sigma^*_{S-Y}$ and $n_X \rightarrow \sigma^*_{S-O}$) induces double bond character between the S and X, while the *exo* anomeric effect ($n_O \rightarrow \sigma^*_{S-X}$) lengthens the S–X bond. In the case of X = NH₂⁺, the *exo* anomeric effect is strengthened and there is no longer a lone pair to engage in the *endo* anomeric effect, as is the case when X = O, leading to an increased S–N bond length. This analysis also explains the shorter bond length when X = O relative to X = NH, despite an increase in p-character, due to the fact two lone pairs are present to partici-

pate in bond-shortening *endo*-anomeric effects. Thus, it is found that more negative interaction energies provided by increased acceptor abilities can either be augmented by favorable remote stereoelectronic effects when X = NH or O or counteracted by bond lengthening and increased distortion energies when X = NH₂⁺, in accordance with Bent's rule.

In a second set of computations (Figure 2A–B), the previously unexplored effects of the homopropargylic Y atom in **10** and **12** was investigated in a similar manner. Because of its remote relationship to the alkyne, this heteroatom was anticipated to have a minimal impact on reactivity; however, experimental and computational findings revealed an unexpected result. Differences in ΔG^\ddagger upon Y heteroatom substitution of CH₂ with O were found to be > 2 kcal/mol; in many cases, the contribution of Y to the lowering of the ΔG^\ddagger neared that of the X heteroatom. This unexpected

[Type here]

increase in reactivity when $Y = O$ or N stems from a decrease in distortion energies due to favorable hybridization and anomeric effects, except in the case of $Y = NH_2^+$.

The picture becomes even more complex when both X and Y heteroatoms are incorporated into the cycloalkyne of **13** (Figure 3), as synergistic effects between the heteroatoms are important to the relative reactivity of the analogs. Overall, heterocycles of the form **13** were found to have increased reactivity over the isolated effects of either X or Y . Because the sulfur must accommodate electronegative atoms at both positions, the p-character utilized by sulfur in bonding orbitals must be split; the higher p-character observed in $S-X$ and $S-Y$ bonds in compounds **11** and 12 is no longer possible. This mediates the bond lengthening and subsequent release of ring strain observed when X or $Y = CH_2$. Thus, incorporation of the sulfamate effectively adjusts the strain of the ring electronically, without the inclusion of sp^2 hybridized groups. This is reflected in the $\Delta E_{\text{distortion}}^\ddagger$ values, which are smaller than those of compounds **11** and 12 , while the $\Delta E_{\text{interaction}}^\ddagger$ values are

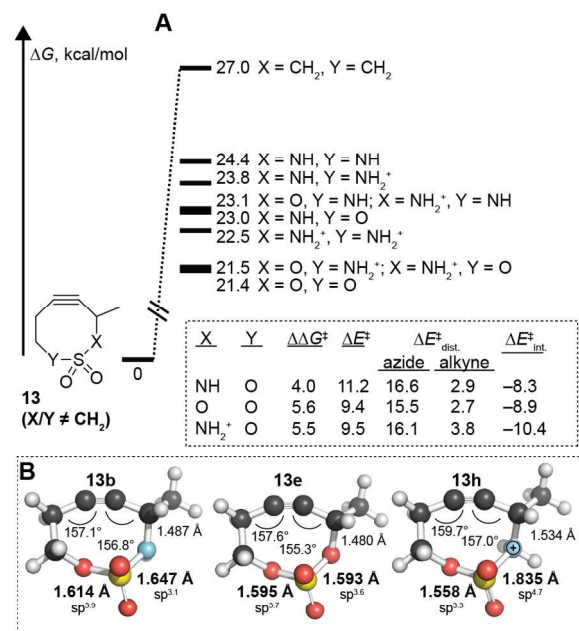


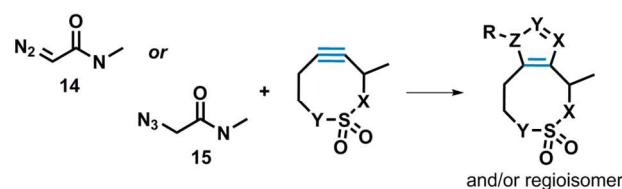
Figure 3. (A) Free energies of activation (kcal/mol) of the lowest energy TSs for cycloadditions of methyl azide with alkynes containing various propargylic and homopropargylic substituents. Geometries were optimized at the M06-2X/6-311+G(d,p) level of theory with an IEFPCM solvent model for water (radii = UFF). **Inset:** $\Delta\Delta G^\ddagger$ relative to $X = Y = CH_2$ and distortion/interaction analysis. For a full analysis and further details, see Tables S6 in the Supporting Information. (B) Starting alkyne geometries with selected bond lengths given in Ångstroms and angles in degrees. Hybridizations were obtained from NBO analysis and are given for sulfur bonding orbitals in $S-Y$ bonds. Black = carbon; white = hydrogen; blue = nitrogen; red = oxygen; yellow = sulfur.

fairly similar. Remote hybridization effects have previously been utilized to increase strain in fused ring systems; this finding provides a new strategy of modulating strain based on the electronic character of remote heteroatoms. Thus, such an approach provides the distinct advantage of enabling the fine-tuning of ring strain

without the steric bulk and synthetic complexity associated with the incorporation of fused rings into the strained cycloalkyne.

Overall, the computationally predicted trend for engaging cooperative effects to increase rates in 1,3-dipolar cycloadditions with MeN_3 indicated that $X/Y = O/O$ should be the most reactive cycloalkyne, followed by $X/Y = NH_2^+/O$ and $X/Y = O/NH_2^+$. Experimental attempts at mimicking $X/Y = NH_2^+/O$ via synthesis of an N -Boc analog **6** (see Table 1) gave a slightly slower rate than $X/Y = NH/O$ in **5**. The failure of Boc incorporation to provide increased reactivity may stem from steric interactions of the Boc group with the neighboring sulfonyl group, thus counteracting the increased acceptor abilities (see the Supporting Information for further details). While the chemistry described in Scheme 1 cannot be employed to afford O in the X position, alternative approaches towards the syntheses of these substrates are currently underway and will be reported in due course.

Table 2. Energies and free energies of activation (kcal/mol) of the lowest energy TSs for each cycloadditions of N -methyl diazo- (**14**) and azidoacetamide (**15**) reacting with alkynes containing various propargylic and homopropargylic substituents. Geometries optimized at the M06-2X/6-311+G(d,p) level of theory with an IEFPCM solvent model for water (radii = UFF). **Bold** indicates compounds that were tested experimentally. ^aIndicates the *syn*-TS is favored. *Syn* refers to the relationship of the R group relative to the C-X bond.



	X	Y	ΔE^\ddagger	ΔG^\ddagger	ΔE^\ddagger	ΔG^\ddagger
11	CH_2	CH_2	15.4	26.9	15.3	27.2
11a	NH	CH_2	13.5	25.8	13.5	25.6
11b	O	CH_2	11.3	21.3	11.6	24.1
11c	NH_2^+	CH_2	11.8	23.2	12.5	24.0
12a	CH_2	NH	13.8	25.0	14.1	26.6
12b	CH_2	O	12.8	24.7	13.0	25.6
12c	CH_2	NH_2^+	14.2 ^a	26.5 ^a	13.7 ^a	25.5 ^a
13a	NH	NH	12.3	24.4	12.5	25.3
13b	NH	O	10.7	21.9	11.5	23.8
13c	NH	NH_2^+	11.3	23.2	12.0	24.8
13d	O	NH	10.1	21.8	10.8	23.5
13e	O	O	8.4	20.2	9.4	21.9
13f	O	NH_2^+	7.9	19.9	9.3	21.8
13g	NH_2^+	NH	10.6	22.5	11.3	23.9
13h	NH_2^+	O	8.6	20.4	9.6	23.4
13i	NH_2^+	NH_2^+	8.9	21.1	10.3	23.8
13j	NBoc	O	10.1	23.1	10.6	24.1

Reaction of alkynes with azides and diazo compounds. More polar transition states were predicted for the reaction of azides with sulfamate-based cycloalkynes by NBO analysis.²⁶ The increased polarity of 1,3-cycloadditions employing diazo groups has been utilized to achieve chemoselective reaction in the presence of competing azide 1,3-dipoles; this tunable selectivity is especially apparent in polar aqueous media.^{5,27} To determine whether our cycloalkynes exhibit similar behavior, reactions of **11**, **12**, and **13** with azidoacetamide **15** and the more polarized diazoacetamide

[Type here]

14 were compared both computationally and experimentally (Table 2 and Figure 4).

Computationally, the difference in ΔG^\ddagger for the two transition states in the reaction of various analogs of **11**, **12**, and **13** with both **14** and **15** were explored (Table 2). When looking at the isolated effects of the X atom (Y = CH₂, **11a–c**), minimal differences were seen for X = NH (**11a**). When X = NH₂⁺ (**11c**), however, a larger gap was observed, due to the increased nucleophilicity of the diazoacetamide **14** compared to that of the azidoacetamide **15**. For both **14** and **15**, a similar decrease in total distortion energies to reach their respective TSs for the reaction with **11c** is observed relative to the reactions with the parent **11** (X = Y = CH₂; $\Delta\Delta E_{\text{dist}}^\ddagger = 1.1$ kcal/mol and 0.7 kcal/mol, respectively). See the Supporting Information for additional details). The alkyne distortion energy increases in both cases, due to geometric considerations that were previously discussed, while both dipole distortions decrease as a result of closer energy FMOs provided by the LUMO-lowering effects of the electronegative propargylic heteroatom. The factor responsible for this differentiation in reactivity also results from FMO considerations, due to the higher energy HOMO of the diazoacetamide **14** relative to the azido analogue **15**.^{5c} This decreased FMO gap results in a much larger interaction energy for the reaction of **14** with **11c** ($\Delta\Delta E_{\text{int}}^\ddagger = -13.8$ kcal/mol) compared to both the reaction of **15** with **11c** ($\Delta\Delta E_{\text{int}}^\ddagger = -10.3$ kcal/mol) and the reactions of **14** and **15** with the parent compound **11** (X = Y = CH₂; $\Delta\Delta E_{\text{int}}^\ddagger = -11.3$ kcal/mol and $\Delta\Delta E_{\text{int}}^\ddagger = -8.2$ kcal/mol, respectively).

Isolating the effects of the Y heteroatoms provides interesting results. For Y = O (**12b**), the diazoacetamide reaction is favored, but interestingly, when Y = NH₂⁺ (**11c**), this trend is reversed and the azide is expected to be favored by a similarly large margin ($\Delta\Delta G^\ddagger = 1.1$ kcal/mol). These results suggest the exciting possibility that alkyne reactivity could be electronically tuned to favor different 1,3-dipoles.

However, when the combined effects of both the X and Y atoms are analyzed, the switch in chemoselectivity is absent. Instead, all of the heteroatom combinations favor reaction with the diazoacetamide **14**. The situation where X = NH and Y = O **13b** gives a $\Delta\Delta G^\ddagger = 1.9$ kcal/mol, while changing to X = NH₂⁺ **13h** gives an even larger preference for reaction with **14** over **15** ($\Delta\Delta G^\ddagger = 3.0$

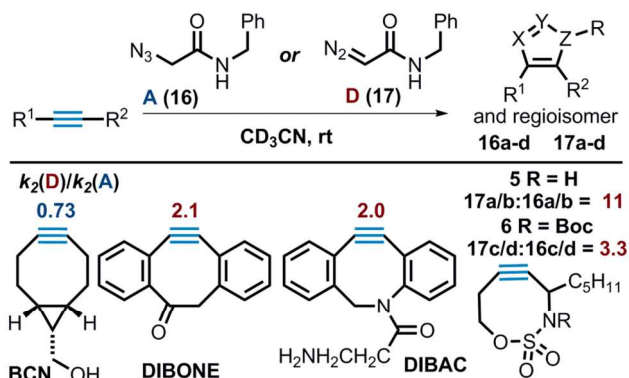


Figure 4. Chemoselectivity in the reaction of strained cycloalkynes with two different 1,3-dipoles.

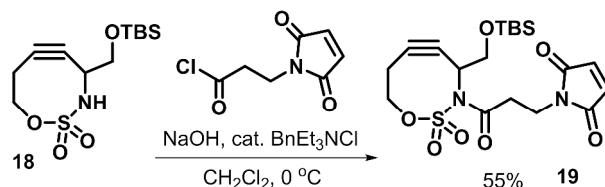
kcal/mol). In the case of **13h**, the more nucleophilic diazoacetamide **14** benefits from the favorable FMO arguments discussed above, without the counter-productive bond-lengthening and relaxation of strain that is seen in compound **11c**. This prediction points to the intriguing possibility of developing bioorthogonal

[Type here]

reactions that employ two or more different 1,3-dipoles with two or more different cycloalkynes to afford mutually orthogonal reactivity.^{1,5,19} Such strategies offer the ability to label various components of complex processes either sequentially^{19a,b,f,h} or simultaneously.^{19c-e,i} While the majority of efforts in this area have utilized the small size of the azide or other dipoles to afford selectivity over the sterically bulky, yet highly reactive tetrazine moiety,^{19c-g,j} few reports of utilizing electronic differences in dipoles⁵ and dipolarophiles^{4g} have been disclosed. Previous reports have shown complete selectivity of diazoacetamides over the analogous azides, however, these systems suffer from either relatively slow reaction kinetics^{5a} or unstable reacting partners,^{5c,f} shortcomings that our new cycloalkyne scaffolds can be employed to overcome with further optimizations.

Experimentally, chemoselectivity was investigated by comparing the rates of reaction of various cycloalkynes with both **A** and **D**, which correspond to the *N*-benzyl acetamide analogues of **14** and **15** (Figure 4). For previous strain-activated alkyne cycloadditions, reported rate differences are minimal, with the best selectivity ~2:1. Gratifyingly, SNO-OCT derivatives **5** and **6** displayed much larger rate differences in the competing 1,3-dipolar cycloadditions with **A** and **D** to yield **16a–b** and **17a–b**, respectively. When X = NBoc, this rate difference for the production of **17c–d** vs. **16c–d** is 3.3:1, but when X = NH, the rate difference between the production of **17a–b** vs. **16a–b** increases to an excellent selectivity of 11:1. As mentioned previously, the Boc group can increase the acceptor properties of the C–N bond, but is not a good mimic of the NH₂⁺ moiety, due to its bulky nature. Efforts to afford both faster reaction kinetics with azides and higher selectivity between both diazo compounds and other reagents utilized in chemical biology are currently underway.

Bioconjugation of SNO-OCT with RNase 1. To assess the utility of SNO-OCTs in a biological context, the maleimide-linked compound **19** was synthesized from **18** (Scheme 2). The primary alcohol of **18** was protected with a TBS silyl ether, as the presence of a free alcohol triggered an *N*- to *O*-acyl shift after amine functionalization; the resulting ester linkage was problematic for bioconjugation studies. Formation of the amide linkage proceeded smoothly to afford **19**. To ensure that the amide linkage did not



Scheme 2. Synthesis of **19**.

significantly affect the rate of 1,3-dipolar cycloaddition, kinetic studies of the reaction of **19** with benzyl azide were carried out in CD₃CN, giving a rate of 0.026 M⁻¹s⁻¹ (see the Supplementary Information for details). The decrease in rate compared to **8** is expected, due to the inclusion of the bulky TBS group, but compares well to the rate seen with our parent SNO-OCT **5**.

To highlight the utility of SNO-OCT **19** in a biological context, we sought to carry out the 1,3-dipolar cycloaddition on a SNO-OCT–protein conjugate. As a model protein, we chose human ribonuclease 1 (RNase 1). Replacement of Pro 19 with Cys provides a variant, P19C RNase 1,²⁸ that allows for facile conjugation to **19**, providing the SNO-OCT–RNase 1 conjugate via the well-established thiol–maleimide conjugation strategy (Figure 5). The

SNO-OCT–RNase 1 conjugate was then reacted with 5 equiv of azide-PEG3-biotin for 2 h at ambient temperature to yield the biotin–RNase 1 conjugate, as confirmed by mass spectrometry (experimental details and mass spec data are contained in the Supporting Information).

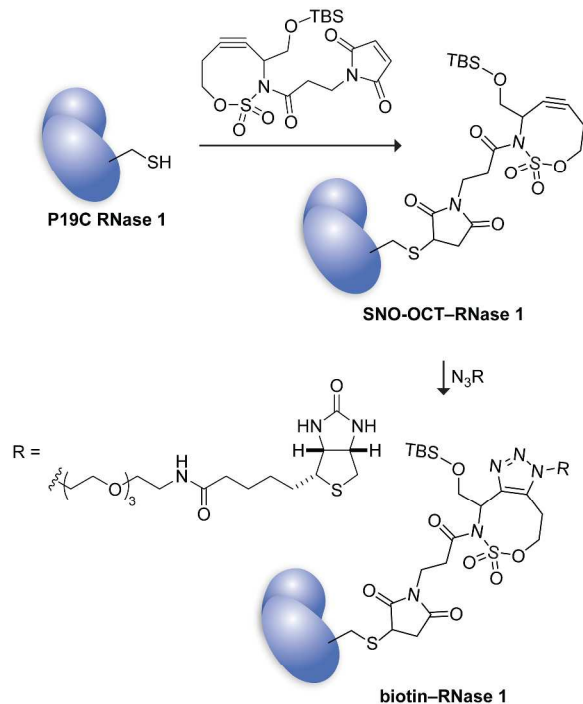


Figure 5. Conjugation of maleimide–SNO-OCT to P19C RNase 1, followed by the 1,3-dipolar cycloaddition of azide-PEG3-biotin.

Conclusion

A mild and efficient synthetic strategy for the preparation of new strained cycloalkynes has been reported. Transition metal-catalyzed aziridination and subsequent ring expansion of a silyl allene precursor delivers the cycloalkyne product, while allowing facile derivatization to modulate the stability, reactivity and/or solubility of these dipolarophiles. The resulting alkynes demonstrated an excellent balance of stability and reactivity; while they were stable to heat, acids and bases, they were still capable of reacting with benzyl azide at rates that outpace previously reported electronically activated alkynes (DIFO, for example). The cooperative effects of the propargylic and homopropargylic heteroatoms, separated by a sulfonyl bridge, provide the opportunity to affect both alkyne electronics and alkyne distortion via remote hybridization and stereoelectronic effects. This adds a new mode of controlling alkyne reactivity, as previous reports have suggested propargylic heteroatoms can alleviate ring strain without sacrificing reactivity. Taken together, these approaches to alkyne design provide principles for the design of highly pre-distorted cycloalkynes that are hyperconjugatively stabilized, yet highly reactive as the interactions in the TS become more important. This mode of electronic activation has also allowed us to achieve rate differentiation between 1,3-dipoles of varying polarity, a step towards the development of highly chemoselective, bioorthogonal methods. The full synthetic potential of these strained alkynes is an area of ongoing investigation in our research groups.

[Type here]

ASSOCIATED CONTENT

Supporting Information

Experimental procedures and spectral data for all new compounds, as well as computational methods and details are supplied in the Supporting Information. This material is available free of charge via the Internet at <http://pubs.acs.org>.

AUTHOR INFORMATION

Corresponding Author

schomakerj@chem.wisc.edu

Author Contributions

#EGB and BG contributed equally to this manuscript.

ACKNOWLEDGMENT

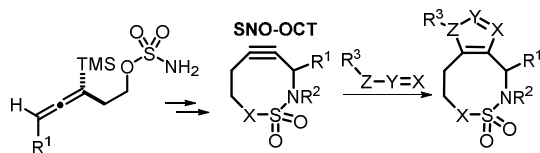
JMS thanks the NIH R01 GM111412 and RTR thanks the NIH R01 GM044783 for funding. BG thanks the Arnold and Mabel Beckman Foundation for support as a Postdoctoral Fellow. The NMR facilities at UW-Madison are funded by NSF (CHE-9208463, CHE-9629688) and NIH (RR08389-01). The National Magnetic Resonance Facility at UW-Madison is supported by NIH (P41GM103399, S10RR08438, S10RR029220) and NSF (BIR-0214394). Computational resources were supported in part by Grant No. CHE-0840494 (NSF). The authors thank Dr. Charles Fry of the University of Wisconsin-Madison for assistance with NMR kinetic studies and Matthew R. Aronoff of the University of Wisconsin for synthesis of the azidoacetamide.

REFERENCES

- For selected general reviews on bioorthogonal labeling, see: a) Lang, K.; Chin, J. W. *ACS Chem. Biol.* **2014**, *9*, 16–20. b) Patterson, D. M.; Nazarov, L. A.; Prescher, J. A. *ACS Chem. Biol.* **2014**, *9*, 592–605. c) Patterson, D. M.; Prescher, J. A. *Curr. Opin. Chem. Biol.* **2015**, *28*, 141–149. d) Debets, M. F.; Van Berkel, S. S.; Dommerholt, J.; Dirks, A. J.; Rutjes, F. P. J. T.; Van Delft, F. L. *Acc. Chem. Res.* **2011**, *44*, 805–815. e) Sletten, E. M.; Bertozzi, C. R. *Angew. Chem. Int. Ed.* **2009**, *48*, 6974–6998. f) Chen, X.; Wu, Y. W. *Org. Biomol. Chem.* **2016**, *14*, 5417–5439.
- a) Nilsson, B. L.; Kiessling, L. L.; Raines, R. T. *Org. Lett.* **2000**, *2*, 1939–1941. b) Saxon, E.; Bertozzi, C. R. *Science* **2000**, *287*, 2007–2010. c) Soellner, M. B.; Dickson, K. A.; Nilsson, B. L.; Raines, R. T. *J. Am. Chem. Soc.* **2003**, *125*, 11790–11791. d) Saxon, E.; Armstrong, J. I.; Bertozzi, C. R. *Org. Lett.* **2000**, *2*, 2141–2143. e) Soellner, M. B.; Nilsson, B. L.; Raines, R. T. *J. Am. Chem. Soc.* **2006**, *128*, 8820–8828.
- Strain as the main method of activation: a) Agard, N. J.; Prescher, J. A.; Bertozzi, C. R. *J. Am. Chem. Soc.* **2004**, *126*, 15046–15047. b) Ning, X.; Guo, J.; Wolfert, M. A.; Boons, G.-J. *Angew. Chem. Int. Ed.* **2008**, *47*, 2253–2255. c) Poloukhine, A. A.; Mbua, N. E.; Wolfert, M. A.; Boons, G.-J.; Popik, V. V. *J. Am. Chem. Soc.* **2009**, *131*, 15769–15776. d) Jewett, J. C.; Sletten, E. M.; Bertozzi, C. R. *J. Am. Chem. Soc.* **2010**, *132*, 3688–3690. e) Dommerholt, J.; Schmidt, S.; Temming, R.; Hendriks, L. J. A.; Rutjes, F. P. J. T.; van Hest, J. C. M.; Lefeber, D. J.; Friedl, P.; van Delft, F. L. *Angew. Chem. Int. Ed.* **2010**, *49*, 9422–9425. f) Mbua, N. E.; Guo, J.; Wolfert, M. A.; Steet, R.; Boons, G.-J. *ChemBioChem* **2011**, *12*, 1912–1921. g) Varga, B. R.; Kallay, M.; Hegyi, K.; Beni, S.; Kele, P. *Chem. Eur. J.* **2012**, *18*, 822–828.
- Strain + electronic effects: a) Baskin, J. M.; Prescher, J. A.; Laughlin, S. T.; Agard, N. J.; Chang, P. V.; Miller, I. A.; Lo, A.; Codelli, J. A.; Bertozzi, C. R. *Proc. Natl. Acad. Sci. U. S. A.* **2007**, *104*, 16793–16797. b) Chenoweth, K.; Chenoweth, D.; Goddard, W. A., III *Org. Biomol. Chem.* **2009**, *7*, 5255–5258. c) Schoenebeck, F.; Ess, D. H.; Jones, G. O.; Houk, K. N. *J. Am. Chem. Soc.* **2009**, *131*, 8121–8133. d) Debets, M. F.; van Berkel, S. S.; Schoffelen, S.; Rutjes, F. P. J. T.; van Hest, J. C. M.; van Delft, F. L. *Chem. Commun.* **2010**, *46*, 97–99. e) Gold, B.; Dudley, G. B.;

- 1 Alabugin, I. V. *J. Am. Chem. Soc.* **2013**, *135*, 1558–1569. f) Garcia-Hartjes, J.; Dommerholt, J.; Wennekes, T.; van Delft, F. L.; Zuilhof, H. *Eur. J. Org. Chem.* **2013**, *2013*, 3712–3720. g) Ni, R.; Mitsuda, N.; Kashiwagi, T.; Igawa, K.; Tomooka, K. *Angew. Chem. Int. Ed.* **2015**, *54*, 1190–1194. h) Dommerholt, J.; van Rooijen, O.; Borrmann, A.; Guerra, C. F.; Bickelhaupt, F. M.; van Delft, F. L. *Nat. Commun.* **2014**, *5*, 5378. i) Jewett, J. C.; Sletten, E. M.; Bertozzi, C. R. *J. Am. Chem. Soc.* **2010**, *132*, 3688–3690.
- 2 5. a) McGrath, N. A.; Raines, R. T. *Chem. Sci.* **2012**, *3*, 3237–3240. b) Andersen, K. A.; Aronoff, M. R.; McGrath, N. A.; Raines, R. T. *J. Am. Chem. Soc.* **2015**, *137*, 2412–2415. c) Gold, B.; Aronoff, M. R.; Raines, R. T. *Org. Lett.* **2016**, *18*, 4466–4469. d) Aronoff, M. R.; Gold, B.; Raines, R. T. *Org. Lett.* **2016**, *18*, 1538–1541. e) Gold, B.; Aronoff, M. R.; Raines, R. T. *J. Org. Chem.* **2016**, *81*, 5998–6006. f) Aronoff, M. R.; Gold, B.; Raines, R. T. *Tetrahedron Lett.* **2016**, *57*, 2347–2350. For further reading on the utilization of diazo compounds in chemical biology see: g) Mix, K. A.; Aronoff, M. R.; Raines, R. T. *ACS Chem. Biol. in press*.
- 3 6. a) Sherratt, A. R.; Chigrinova, M.; MacKenzie, D. A.; Rastogi, N. K.; Ouattara, M. T. M.; Pezacki, A. T.; Pezacki, J. P. *Bioconjugate Chem.* **2016**, *27*, 1222–1226. b) Temming, R. P.; Eggermont, L.; van Eldijk, M. B.; van Hest, J. C. M.; van Delft, F. L. *Org. Biomol. Chem.* **2013**, *11*, 2772–2779. c) McKay, C. S.; Blake, J. A.; Cheng, J.; Danielson, D. C.; Pezacki, J. P. *Chem. Commun.* **2011**, *47*, 10040–10042. d) Ning, X.; Temming, R. P.; Dommerholt, J.; Guo, J.; Blanco-Ania, D.; Debets, M. F.; Wolfert, M. A.; Boons, G.-J.; Van Delft, F. L. *Angew. Chem. Int. Ed.* **2010**, *49*, 3065–3068.
- 4 7. a) Stöckmann, H.; Neves, A. A.; Stairs, S.; Brindle, K. M.; Leeper, F. J. *Org. Biomol. Chem.* **2011**, *9*, 7303–7305. b) Wang, Y.; Song, W.; Hu, W. J.; Lin, Q. *Angew. Chem. Int. Ed.* **2009**, *48*, 5330–5333. c) Yu, Z.; Pan, Y.; Wang, Z.; Wang, J.; Lin, Q. *Angew. Chem. Int. Ed.* **2012**, *51*, 10600–10604.
- 5 8. Yarema, K. J.; Mahal, L. K.; Bruehl, R. E.; Rodriguez, E. C.; Bertozzi, C. R. *J. Biol. Chem.* **1998**, *273*, 31168–31179.
- 6 9. a) McGrath, N. A.; Andersen, K. A.; Davis, A. K. F.; Lomax, J. E.; Raines, R. T. *Chem. Sci.* **2015**, *6*, 752–755. b) Mix, K. A.; Raines, R. T. *Org. Lett.* **2015**, *17*, 2359–2361.
- 7 10. a) Blackman, M. L.; Royzen, M.; Fox, J. M. *J. Am. Chem. Soc.* **2008**, *130*, 13518–13519. b) Darko, A.; Wallace, S.; Dmitrenko, O.; Machovina, M. M.; Mehl, R. A.; Chin, J. W.; Fox, J. M. *Chem. Sci.* **2014**, *5*, 3770–3776. c) Selvaraj, R.; Giglio, B.; Liu, S.; Wang, H.; Wang, M.; Yuan, H.; Chintala, S. R.; Yap, L. P.; Conti, P. S.; Fox, J. M.; Li, Z. *Bioconjugate Chem.* **2015**, *26*, 435–442. Tetrazine–cyclopropene: d) Yang, J.; Šeckute, J.; Cole, C. M.; Devaraj, N. K. *Angew. Chem. Int. Ed.* **2012**, *51*, 7476–7479. e) Patterson, D. M.; Nazarova, L. A.; Xie, B.; Kamber, D. N.; Prescher, J. A. *J. Am. Chem. Soc.* **2012**, *134*, 18638–18643. f) Kamber, D. N.; Nazarova, L. A.; Liang, Y.; Lopez, S. A.; Patterson, D. M.; Shih, H.-W.; Houk, K. N.; Prescher, J. A. *J. Am. Chem. Soc.* **2013**, *135*, 13680–13683. g) Yang, J.; Liang, Y.; Šeckute, J.; Houk, K. N.; Devaraj, N. K. *Chem. Eur. J.* **2014**, *20*, 3365–3375. h) Sachdeva, A.; Wang, K.; Elliott, T.; Chin, J. W. *J. Am. Chem. Soc.* **2014**, *136*, 7785–7788. i) Kamber, D. N.; Liang, Y.; Blizzard, R. J.; Liu, F.; Mehl, R. A.; Houk, K. N.; Prescher, J. A. *J. Am. Chem. Soc.* **2015**, *137*, 8388–8391.
- 8 11. a) van Berkel, S. S.; Dirks, A. J.; Debets, M. F.; van Delft, F. L.; Cornelissen, J. J. L. M.; Nolte, R. J. M.; Rutjes, F. P. J. T. *ChemBioChem* **2007**, *8*, 1504–1508. b) Gutmiedl, K.; Wirges, C. T.; Ehmke, V.; Carell, T. *Org. Lett.* **2009**, *11*, 2405–2408. c) Sletten, E. M.; Bertozzi, C. R. *J. Am. Chem. Soc.* **2011**, *133*, 17570–17573. d) Wright, T. H.; Bower, B. J.; Chalker, J. M.; Bernardes, G. J. L.; Wiewiora, R.; Ng, W.-L.; Raj, R.; Faulkner, S.; Vallee, R. J.; Phnumartwiwath, A.; Coleman, O. D.; Thezenas, M.-L.; Khan, M.; Galan, S. R. G.; Lercher, L.; Schombs, M. W.; Gerstberger, S.; Palm-Espling, M. E.; Baldwin, A. J.; Kessler, B. M.; Claridge, T. D. W.; Mohammed, S.; Davis, B. G. *Science*, **2016**, *354*, 597.
- 9 12. a) Pigge, F. C. *Curr. Org. Chem.* **2016**, *20*, 1902–1922. b) Del Amo, D. S.; Wang, W.; Jiang, H.; Besanceney, C.; Yan, A. C.; Levy, M.; Liu, Y.; Marlow, F. L.; Wu, P. *J. Am. Chem. Soc.* **2010**, *132*, 16893–16899. c) Wolbers, F.; ter Braak, P.; Le Gac, S.; Luttge, R.; Andersson, H.; Vermes, I.; van den Berg, A. *Electrophoresis* **2006**, *27*, 5073–5080. d) Link, A. J.; Tirrell, D. A. *J. Am. Chem. Soc.* **2003**, *125*, 11164–11165.
- 10 13. a) Blomquist, A. T.; Liu, L. H. *J. Am. Chem. Soc.* **1953**, *75*, 2153–2154. b) Wittig, G.; Krebs, A. *Chem. Ber.* **1961**, *94*, 3260–3275.
- 11 14. a) Munster, N.; Nikodemski, P. Koert, U. *Org. Lett.* **2016**, *18*, 4296–4299. b) Binder, W. H.; Sachsenhofer, R. *Macromol. Rapid Commun.* **2007**, *28*, 15–54.
- 12 15. Heber, D.; Rosner, P.; Tochtermann, W. *Eur. J. Org. Chem.*, **2005**, 4231–4247.
- 13 16. van Geel, R.; Pruijij, G. J. M.; van Delft, F. L.; Boelens, W. C. *Bioconjugate Chem.* **2012**, *23*, 392–398.
- 14 17. a) Gold, B.; Shevchenko, N. E.; Bonus, N.; Dudley, G. B.; Alabugin, I. V. *J. Org. Chem.* **2012**, *77*, 75–89. b) Gold, B.; Batsomboon, P.; Dudley, G. B.; Alabugin, I. V. *J. Org. Chem.* **2014**, *79*, 6221–6232. c) Ni, R.; Mitsuda, N.; Kashiwagi, T.; Igawa, K.; Tomooka, K. *Angew. Chem. Int. Ed.* **2015**, *54*, 1190–1194. d) Kaneda, A.; Naruse, R.; Yamamoto, S. *Org. Lett.*, **2017**, *19*, 1096–1099.
- 15 18. Mayr, H.; Ofial, A. R.; *Angew. Chem. Int. Ed.* **2006**, *45*, 1844–1854.
- 16 19. a) Sanders, B. C.; Friscourt, F.; Ledin, P. A.; Mbua, N. E.; Arumugam, S.; Guo, J.; Boltje, T. J.; Popik, V. V.; Boons, G.-J. *J. Am. Chem. Soc.* **2011**, *133*, 949–957. b) Willems, L. I.; Li, N.; Florea, B. I.; Ruben, M.; van der Marel, G. A.; Overkleeft, H. S. *Angew. Chem. Int. Ed.* **2012**, *51*, 4431–4434. c) Karver, M. R.; Weissleder, R.; Hilderbrand, S. A. *Angew. Chem. Int. Ed.* **2012**, *51*, 920–922. d) Plass, T.; Milles, S.; Koehler, C.; Szymański, J.; Mueller, R.; Wiebler, M.; Schultz, C.; Lemke, E. A. *Angew. Chem. Int. Ed.* **2012**, *51*, 4166–4170. e) Patterson, D. M.; Nazarova, L. A.; Xie, B.; Kamber, D. N.; Prescher, J. A. *J. Am. Chem. Soc.* **2012**, *134*, 18638–18643. f) Liang, Y.; Mackey, J. L.; Lopez, S. A.; Liu, F.; Houk, K. N. *J. Am. Chem. Soc.* **2012**, *134*, 17904–17907. g) Kamber, D. N.; Nazarova, L. A.; Liang, Y.; Lopez, S. A.; Patterson, D. M.; Shih, H.-W.; Houk, K. N.; Prescher, J. A. *J. Am. Chem. Soc.* **2013**, *135*, 13680–13683. h) Cole, C. M.; Yang, J.; Šeckute, J.; Devaraj, N. K. *ChemBioChem* **2013**, *14*, 205–208. i) Sachdeva, A.; Wang, K.; Elliott, T.; Chin, J. W. *J. Am. Chem. Soc.* **2014**, *136*, 7785–7788. j) Narayanan, M. K.; Liang, Y.; Houk, K. N.; Murphy, J. M. *Chem. Sci.* **2016**, *7*, 1257–1261.
- 17 20. Tummatorn, J.; Batsomboon, P.; Clark, R. J.; Alabugin, I. V.; Dudley, G. B. *J. Org. Chem.* **2012**, *77*, 2093–2097.
- 18 21. Gregg, T. M.; Farrugia, M. K.; Frost, J. R. *Org. Lett.* **2009**, *11*, 4434–4436.
- 19 22. Burke, E. G.; Schomaker, J. M. *Angew. Chem. Int. Ed.* **2015**, *54*, 12097–12101.
- 20 23. a) Ess, D. H.; Houk, K. N. *J. Am. Chem. Soc.* **2008**, *130*, 10187–10198. b) For a tutorial review of the distortion/interaction model (which is also known as the activation-strain model), see: Fernandez, I.; Bickelhaupt, F. M. *Chem. Soc. Rev.* **2014**, *43*, 4953–4967. c) Wolters, L. P.; Bickelhaupt, F. M. *WIREs Comput. Mol. Sci.* **2015**, *5*, 324–343.
- 21 24. a) Bent, H. A. *J. Chem. Phys.* **1959**, *33*, 1258–1259. b) Bent, H. A. *J. Chem. Ed.* **1960**, *37*, 616–624. c) Bent, H. A. *Chem. Rev.* **1961**, *61*, 275–311. d) Alabugin, I. V.; Bresch, S.; Gomes, G. *J. Phys. Org. Chem.* **2015**, *28*, 147–162. e) Alabugin, I. V.; Bresch, S.; Mariappan, M. *J. Phys. Chem. A* **2014**, *118*, 3663–3677.
- 22 25. a) Szarek, W. A.; Horton, D.; Eds. *The Anomeric Effect: Origin and Consequences*; ACS Symposium Series No. 87; American Chemical Society: Washington, DC; **1979**. b) Kirby, A. J. *The Anomeric Effect and Related Stereoelectronic Effects at Oxygen*; Springer: New York, 1983. c) Juaristi, E.; Cuevas, G. *The Anomeric Effect*; CRC Press: Boca Raton; **1995**. d) Thatcher, G. R. J.; Ed. *The Anomeric Effect and Associated Stereoelectronic Effects*; ACS Symposium Series No. 539; American Chemical Society: Washington, DC; **1993**. e) Alabugin, I. V. *Stereoelectronic Effects: a bridge between structure and reactivity*; Wiley: Chichester, **2016**. f) Alabugin, I. V.; Gold, B. in *Encyclopedia of Physical Organic Chemistry*; Wang, Z., Ed.; Wiley: Chichester, **2017**.
- 23 26. Glendening, E. D.; Badenhop, J. K.; Reed, A. E.; Carpenter, J. E.; Bohmann, J. A.; Morales, C. M.; Landis, C. R.; Weinhold, F. NBO 6.0; Theoretical Chemistry Institute, University of Wisconsin: Madison, WI, **2013**.
- 24 27. a) Breslow, R. *Acc. Chem. Res.* **1991**, *24*, 159–164. b) Meijer, A.; Otto, S.; Engberts, J. B. F. N. *J. Org. Chem.* **1998**, *63*, 8989–8994. c) Narayan, S.; Muldoon, J.; Finn, M. G.; Fokin, V. V.; Kolb, H. C.; Sharpless, K. B. *Angew. Chem. Int. Ed.* **2005**, *44*, 3275–3279. d) Chandrasekhar, J.; Shariffskul, S.; Jorgensen, W. L. *J. Phys. Chem. B* **2002**, *106*, 8078–8085. e) Ess, D. H.; Jones, G. O.; Houk, K. N. *Adv. Synth. Catal.* **2006**, *348*, 2337–2361. f) Jung, Y.; Marcus, R. A. *J. Am. Chem. Soc.* **2007**, *129*, 5492–5502.
- 25 28. Johnson, R. J.; Chao, T.-Y.; Lavis, L. D.; Raines, R. T. *Biochemistry*, **2007**, *46*, 10308–10316.

[Type here]



Faster rates than DIFO *Stable under acidic and basic conditions*
Unreactive with glutathione *Water-soluble*
Significant rate differentiation between azides and diazos

13
14
15
16
17
18
19
20
21
22
23
24
25
26
27
28
29
30
31
32
33
34
35
36
37
38
39
40
41
42
43
44
45
46
47
48
49
50
51
52
53
54
55
56
57
58 [Type here]
59
60